

HHS Public Access

Author manuscript

J Am Soc Mass Spectrom. Author manuscript; available in PMC 2022 June 06.

Published in final edited form as:

J Am Soc Mass Spectrom. 2022 June 01; 33(6): 944–951. doi:10.1021/jasms.2c00004.

Comparing Selected-Ion Collision Induced Unfolding (CIU) with All Ion Unfolding (AIU) Methods for Comprehensive Protein Conformational Characterization

Ashley Phetsanthad¹, Gongyu Li^{2,*}, Chae Kyung Jeon³, Brandon T. Ruotolo³, Lingjun Li^{1,*}

¹Department of Chemistry and School of Pharmacy, University of Wisconsin-Madison, Madison, WI 53705 USA

²Research Center for Analytical Science and Tianjin Key Laboratory of Biosensing and Molecular Recognition, College of Chemistry, Nankai University, Tianjin 300071, China

³Department of Chemistry, University of Michigan, Ann Arbor, MI 48109, USA

Abstract

Structural analysis by native ion mobility-mass spectrometry provides a direct means to characterize protein interactions, stability, and other biophysical properties of disease-associated biomolecules. Such information is often extracted from collision-induced unfolding (CIU) experiments, performed by ramping a voltage used to accelerate ions entering a trap cell prior to an ion mobility separator. Traditionally to simplify data analysis and achieve confident ion identification, precursor ion selection with a quadrupole is performed prior to collisional activation. Only one charge state can be selected at one time, leading to an imbalance between the total time required to survey CIU data across all protein charge states and the resulting structural analysis efficiency. Furthermore, the arbitrary selection of a single charge state can inherently bias CIU analyses. We herein aim to compare two conformation sampling methods for protein gas-phase unfolding: 1) traditional quadrupole selection-based CIU, 2) non-targeted, charge selection-free and shotgun workflow, all ion unfolding (AIU). Additionally, we provide a new data interpretation method that integrates across all charge states to project collisional cross section (CCS) data acquired over a range of activation voltages to produce a single unfolding fingerprint, regardless of charge state distributions. We find that AIU in combination with CCS accumulation across all charges offers an opportunity to maximize protein conformational information with minimal time cost, where additional benefits include: 1) an improved signal to noise ratios for unfolding fingerprints, and 2) a higher tolerance to charge state shifts induced by either operating parameters or other factors that affect protein ionization efficiency.

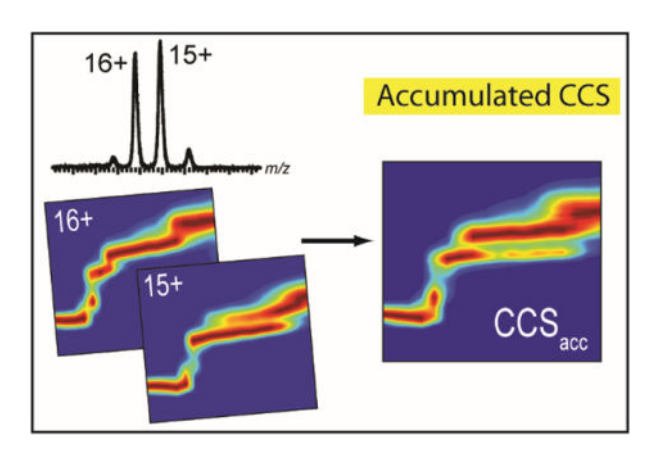
Graphical Abstract

α-chymotrypsin (Figure S2), LTF (Figure S3), OVA (Figure S4) and IgG (Figure S5).

^{*}Corresponding authors: Prof. Dr. Gongyu Li, ligongyu@nankai.edu.cn; Prof. Dr. Lingjun Li, lingjun.li@wisc.edu.

The Supporting Information is available free of charge at https://pubs.acs.org/doi/...

Additional details for CCS accumulation procedure, charge state shift day-by-day evidence (Figure S1), CCSacc unfolding results for



Accumulation of structural information gathered from several charge states allows for a more wholistic view on overall protein characterization.

INTRODUCTION

Ion mobility-mass spectrometry (IM-MS) techniques are continuously improving and being more widely recognized as useful tools for probing the structure and stability of biomolecules such as lipids, peptides, proteins, and large protein complexes 1-6. The ability to couple ion mobility spectrometry (IMS) with various ionization techniques, such as electrospray ionization (ESI) and matrix-assisted laser desorption/ionization (MALDI)⁷, makes it very versatile in its applications. IMS acts as a method of separation, enabling the differentiation of compounds with identical m/z values by exploiting the differences in gasphase conformation and charge state⁸. The resulting drift time measured can be translated to a collisional cross section (CCS) value that corresponds with the size or conformation of the analyte. Studying the changes in CCS values in response to unfolding by applying collision energy (CE) to the gas phase analytes provides increased structural details in a technique called collision induced unfolding (CIU). CIU is a gas-phase tool that induces the stepwise unfolding of proteins and provides information about the unfolding pathway, stability, domains, and binding dynamics of target proteins^{9–12}. Commonly, a precursor ion is selected and energy is applied to gradually unfold a protein to eventually produce a fingerprint contour plot, although the precursor either must be carefully selected or be screened at the significant cost of time, as different unfolding transitions and pathway can be observed depending on the charge state of the selected precursor ion¹¹.

ESI allows for the production of intact multiply charged ions in the gas phase resulting from varying degrees of protonation at each available basic site^{13–14}. The presence of multiple charge states can be partially attributed to multiple conformations of gas phase ions, due to a difference in solvent/proton accessible surface area^{15–19}, along with other factors including solvent pH, composition and gas phase interactions^{20–26}. Such factors are often considered when selecting a charge state for CIU analysis; observing different protein conformations based on ion selection can lead to biased analyses. The correlation between observed gas phase conformation and bulk solution phase structure has been studied extensively^{14, 24, 27–35}. It has been suggested that the CCS data extracted from lower

charge state conformations can be more easily linked to native-like protein conformations³⁶. While there is some consensus that there may be a relationship between the charge state distribution of a compound in the gas phase and in solution, that distribution is likely not fully representative of the solution-phase charge states²⁴, ²⁹, ³¹, ³⁷–³⁹. However, through careful selection of solution conditions and instrument parameters, bulk solution protein structure can be well preserved into the gas phase and translated into the observed gas-phase charge states³⁸.

Although charge-separated CCS distributions represent rich structural information in the gas phase, specific evidence that would allow for the prediction of those protein ion charge states that carry the most native-like structure information remains largely illusive. To facilitate surveying CIU data for the most differentiating charge state, an alternative would be to record unfolding data for all protein charge states achieved in a quadrupole selection-free, All Ion Unfolding (AIU), approach. When removing quadrupole ion filtering, protein activation mass spectra and corresponding unfolding trajectories are collected over a broad m/z range as a function of collision energy. By bypassing precursor ion selection during data acquisition, operator and instrument time required are decreased drastically. While less common in the broad field of protein investigation, we would like to mention that AIU has been routinely employed to study membrane proteins^{40–42}, as well as in instances where quadrupole selection is not possible prior to collisional activation in the drift cell due to instrument configuration^{9, 43–44}. While the use of AIU and All Ion Fragmentation (AIF) schemes are being increasingly applied to improve structural characterization, when appropriate, there remains a need to better incorporate the large amount of information gathered. AIU operation retains information from all ion structures, although the data is commonly analyzed in a charge-separated mode. A recent study by Polasky et al. addressed the need for a method to combine multi-charge state structural information, leading to the development of an algorithm to build multi-state protein classifiers and improving the accuracy of single-state classifiers⁴⁵. While a plethora of information can be retained through traditional IM-MS analysis, data integration methods to visualize all protein structural information in a single unfolding fingerprint has not yet been evaluated as a tool for protein analysis.

Here, as shown in Figure 1, we first compare the effects of quadrupole selection on the performance of unfolding and its resultant data quality. Then we introduce an accumulative CCS accumulation approach for unfolding data interpretation with a novel CCS reporting parameter, accumulated CCS (CCS_{acc}), which sums data across all observed charge states to better differentiate gas-phase protein structures and conformations. We find that the unfolding difference plots generated using this CCS_{acc} approach are more robust, with a higher tolerance to shifts in the protein charge states produced during nESI. Additionally, we observe an increase in overall signal intensity captured for comparisons, also leading to improved unfolding fingerprint quality. Notably, this CCS_{acc} approach retains charge-separated CIU information, which can be extracted on demand as well.

EXPERIMENTAL

Chemicals.

Protein samples (including albumin from chicken egg white (ovalbumin), transferrin, cytochrome c, bovine/human serum albumin, lactotransferrin, beta-lactoglobulin and concanavalin A) and necessary buffer salts were obtained from Sigma-Aldrich (St. Louis, MO). No further purification was performed for the reagents. All solvents used in this study were of HPLC grade supplied by Sigma-Aldrich (St. Louis, MO). Purified water (conductivity of 18.2 M Ω .cm) was obtained from a Milli-Q $\mathbb R$ Reference System (Millipore Corp., Bedford, MA, USA).

IM-MS Experiments.

A homemade nanoelectrospray ion source was used, consisting of a platinum wire of 100 µm thickness inserted into a borosilicate glass needle pulled in house via a P-2000 laser-based micropipette puller (Sutter Instruments, Novato, CA, USA). A volume of 6 μL (~8 μM proteins in 100 mM ammonium acetate) was loaded and nanospray voltages ranging from 1.2 to 1.8 kV was applied with a sampling cone voltage of 30 V and MS cone temperature of 70 °C to preserve native conformation. Backing pressure in the source region was maintained at ~6 mbar, the traveling wave ion mobility separator at ~3.5 mbar, the DC voltage waves at 30 V and the traveling wave height at 400 m/s. The MS instrument was typically operated over the m/z 400 - m/z 8000. All data were acquired on a Waters Synapt G2 instrument (Waters Corporation, Milford, MA, USA) in positive ion mode for mobility acquisition and all unfolding experiments were carried out by altering the trap CE from 10 V to 180 V with a step voltage of 10 V. The analysis of cytochrome c was carried out using a step size of 5 V. Origin (OriginLab Corporation, Northampton, MA, USA) was used to accumulate CCS profiles. The CIUSuite2 data analysis software package was extensively used to create CIU fingerprint heatmaps and calculate root-mean-square deviation (RMSD) values between these maps.

Data Analysis.

As ions of differing charge states experience differing internal ion energy, CE values are converted to lab-frame CE for more appropriate comparisons⁴⁶. CCS calibration curves were generated using a previously described protocol, and using literature CCS values with nitrogen (N₂) derived for use with the Synapt instrument platform^{8, 47}. As CCS values rely on the ion mass, this must be performed separately for each ion. For CCS accumulation, CCS_{acc} is accomplished first by interpolating acquired unfolding datasets (Step 1–2). Following CCS interpolation, all unfolding datasets are then normalized separately (Step 3), and then integrated together based on their relative abundance as shown in the starting native MS1 spectrum (Step 4). We developed a software package, AIUCat, in order to calculate the relative intensity for each charge state at each lab-frame CE and automatically accumulate all CCS datasets (Step 5–6). See Supplementary Information for a more detailed procedure. The subsequent data is then used for further CIUSuite software visualization.

Comparative AIU and CIU Experiments.

Parallel CIU and AIU workflows are shown in Figure 1. In CIU workflows, data acquisition typically begins with a preliminary MS1 scan to observe the protein signals of interest, followed by quadrupole ion filtering to select the desired charge state. CIU is then performed through increasing the applied activation energy in a stepwise format. If more than one charge state unfolding profile is desired, this process can be repeated for each subsequent charge state. For the AIU workflow, precursor ion selection is omitted and all ions in a wide mass range are subjected for collisional unfolding, in a non-targeted activation mode. This workflow critically relies on the integration of structural information from all observed charge states in one parameter, CCS_{acc}. This accumulated data is then ready for further visualization and quantitative analysis. This, in combination with the acceleration voltage required to convert 50% of a protein conformer into its adjacent, CCS-resolved conformational state observed within charge state-integrated data (CIU50_{acc}) can be used to perform quantitative comparisons among fingerprints under various conditions 48–49.

RESULTS AND DISCUSSION

AIU and CIU Comparison.

Many prior results in IM-MS community have indicated that CIU data acquired from different protein charge states carry varying information of conformational stability, unfolding fingerprint transition numbers and characteristic unfolding features. Figure S1a illustrates the comparative native IM-MS spectra of bovine serum albumin (BSA), as acquired for four separate days. It was observed with considerable variations of charge state distributions across different days, where the center charge state unintentionally varied from 17+ to 15+. Additionally, we also compared the unfolding fingerprints for BSA obtained through CIU and AIU. We firstly observed similar trends for charge state-dependent unfolding pathways (Figures S1b-c) for both AIU and CIU datasets. Significant changes were observed in the underlying conformational information as extracted from the shifts in charge states. Likewise, the difference plots (Figure S1d) for AIU and CIU fingerprints with relatively undiscriminating RMSD values ranging from ~8% to ~10% for charges from 16+ to 18+, respectively. The differences observed between CIU data collected for each charge state indicate a need to retain structural/conformational information from all ions across differing charge states. Additionally, this observation indicates an emerging need to integrate the data and treat CIU data collected across all charge states as a different class of information when compared to single charge state CIU.

CCS_{acc} Proof-of-Concept Application on Serum Albumin.

The integration of native-like CCS data provides a rich set of information from which to compare proteins. This is performed by integrating all charge (or at least major charge states) structural information into a single parameter that counts the abundance information through CCS accumulation with the provided AIUCat package. It is beneficial for AIUCat to include the space of relative intensity of individual charge states, as different charge states not only carry distinct structural information, but also contribute in different ratios to the overall protein populations. For the example of HSA, the detailed CCS accumulation function is illustrated in Figure 2a, using the relative abundance of the charge states in the

acquired spectra of HSA (Figure 2b). Upon executing this accumulation function to all lab-frame CEs and all interpolated CCS data points, the accumulated CCS distributions shown in Figure 2a, with select representative collision voltages, are visualized. The individual CCS_{acc} profiles displayed exemplifies differences in CCS values for each charge state and the accumulated profile across the increasing energies. This demonstrates the structure dependence due to observed charge state and the ability to consider structural contribution from each ion through CCS_{acc} profiles. CCS_{acc}, the all-encompassing gas phase ion profile, is seen in red. Considering the relative contributions from each charge state species allows for an overall view of the existing HSA structure heterogeneity.

A new unfolding fingerprint can be created from the calculated CCS_{acc} data of HSA and is compared with the two dominant charge state configurations of HSA, 16+ and 15+ (Figure 2c). Overall, this CCS_{acc} fingerprint shows a 9.80% RMSD difference from the most abundant 16+ fingerprint and a 21.01% difference from the second most abundant charge state of 15+. As 16+ has the highest relative abundance, it had the largest contribution to the CCS_{acc} fingerprint, accounting for the larger discrepancy between the fingerprint of 15+. However, with a RMSD value of 9.80%, the contribution of 15+ and 14+ charge states show a change in the fingerprint characterizing HSA as a whole. This demonstrates the loss of information and that would have occurred if only single charge state data was analyzed and not incorporated with all information gathered. Additionally, when comparing the two abundant species 16+ and 15+, the CCS_{acc} fingerprint holds even more striking domain-informative, three-transition unfolding feature (Figure 3a). The resultant conformational stability information as revealed by CIU₅₀ values also shows differences between accumulated fingerprints and single charge state fingerprint, further highlighting the necessity of considering all charge state structural information, as a complementary data reporting method to conventional unfolding-based native IM-MS structural probing approaches.

AIU and CCS_{acc} -based Comprehensive Conformational Comparison of Structurally Similar Serum Albumins.

AIU fingerprints in combination with CCS_{acc} data processing can be employed to more comprehensively elucidate conformational differences between protein species variants. To demonstrate this, we acquired AIU data for both BSA and HSA, and then extracted CCS_{acc} dataset followed by quantitative analysis with CIUSuite software. Eschweiler et al. similarly interrogated the unfolding differences between serum albumin originating from various species, however their comparisons and observations were made at the single charge state level⁵⁰. For both proteins, nESI-MS under native conditions produces several charge states (Figure 2b), which we interrogated using AIU (Figure 3). We detect significant differences between HSA (Figures 3a–e) and BSA (Figures 3f–j) unfolding data across all charge states quantified in the RMSD values recorded for fingerprint comparisons conducted for each charge state observed, ranging from 10.71–12.81%, as shown in the difference plots of Figures 3k–o. Figure 3p shows similar feature CCS distributions observed between BSA and HSA at each charge state, however between charge states, observed features differ.

In Figure 3q, unambiguous CIU₅₀ values for BSA and HSA are shown when accumulated, although single charge state values will lead to different conclusions being drawn through the comparison of the two species depending on the selected charge state. CIU₅₀ values describe the point at which enough energy is applied to activate 50% of a protein to its next transition state. However, without considering the different gas-phase ions present, that value for 50% cannot be applied wholistically to describe a protein. By considering the all ions of each protein, a CIU₅₀ value can be determined to describe the point where 50% of observed gas-phase ions reach the next transition state. This enables an overall increase in protein distinguishing CIU₅₀ values. While no significant difference in CIU₅₀ values were observed with the most biologically relevant (due to agreement between protein domains and observed number of features⁵¹) charge state of 16+ (delta CIU₅₀1, ~2 eV; delta CIU₅₀2, ~24 eV), the CCS accumulation enables the differentiation between HSA and BSA by 85 eV and 108 eV, for delta CIU₅₀1 and delta CIU₅₀2, respectively. Thus, CCS accumulation empowers the unfolding fingerprint-based structural differentiation of structurally similar proteins with improved structure differing information by elevation of around ~6%-9% CIU50 values (HSA: CIU₅₀1/CIU₅₀2, 857 eV/1360 eV).

Depending on the selected charge state to characterize the differences between BSA and HSA unfolding fingerprints, the RMSD values differ (Figure 3r), with an average RMSD of 11.8% and variations of ~9% between values. These RMSD values not only represent conformational differences between HSA and BSA, but also suggest the presence of charge state bias for conformational comparisons, given the fact that RMSD deviations are higher than commonly observed baseline RMSDs (e.g. for BSA 16+ triplicates being of 6.7%, data not shown). There is uncertainty of using a single charge state to represent whole protein conformations. After integrating the charge-resolved data, the CCS_{acc} profiles of HSA and BSA were compared, and we observe an RMSD of 13.60%. This is an approximately 6% increase in RMSD values of the differences associated between HSA and BSA, and thus comparison capabilities, than if the most distinguishing charge state of 17+ was interrogated alone (RMSD 12.81%).

Collectively, data from both CIU50-based conformational stability comparisons and RMSD-based overall unfolding fingerprint comparisons clearly demonstrated that, AIU and CCS accumulation enables more structurally informative conformational comparisons and comprehensive characterization for subtle structural differences of biologically similar proteins.

AlU and CCS_{acc}-based Comprehensive Conformational Analysis of Sialylated Transferrin and Other Proteins.

We then applied CCS_{acc} to a sialylated glycoprotein, bovine transferrin (bTF), to testify its potential utility to rapidly probe the glycosylation effects on protein structures. A representative native mass spectrum for bTF is shown in Figure 4a along with corresponding drift time heatmap, where four major charge states (more than 5% each) can be assigned from 20+ to 17+. Notably, as a glycoprotein with at least two N-glycosylation residues as evidenced by previous glycan studies⁵², transferrin is a heterogenous protein with multiple

glycoforms and our native MS data in Figure 4a clearly support the presence of multiple glycoforms.

Next, we tracked the stepwise unfolding behavior of bTF (Figures 4b–e) with the AIU operation mode. The first conformer for differing charge states display a variety of CCS values ranging from 57.23 nm² to 59.75 nm². Generally, ions of four charge states carry two major conformational transitions but with some noticeable differences in unfolding pathway. For example, ion of 17+ has one short-lived conformational intermediate with median CCS of 67.79 nm² and ion of 18+ seems to simultaneously adopt two conformers (median CCSs: 82.21 nm² and 88.82 nm²) at the late unfolding stage. Figure 4f shows the typical accumulated unfolding fingerprints as derived through CCS_{acc}. It is clearly observed that four distinct conformers dominate the bTF unfolding process, with median CCSs of ~58 nm², ~71 nm², ~73 nm² and ~89 nm², respectively. Compared to the most abundant single charge state (19+), the major unfolding conformers bear almost the same median CCS values (Figure 4f vs Figure 4d), except that new conformational feature (#2, \sim 71 nm²) observed in CCSacc fingerprint. Furthermore, the overall difference between accumulated CCS-based unfolding and most abundant charge (19+) unfolding had a RMSD value of 13.35% (Figure 4g). CCS_{acc} bridges the structural discrepancies observed from different ion species, as shown in Figures 4h-i. Moreover, conformational feature CCS analysis and corresponding CIU50-based stability analysis reveal that, CCS_{acc}-derived datasets surprisingly do not match best to that of most abundant charge state, which is frequently and arbitrarily used in traditional CIU analysis. These differences should be primarily originated from the contribution of ion species other than the most abundant one, and the observations highlight the potential bias and/or structural loss by using single charge as a structural signature of the whole protein species in solution. Thus, we conclude CCS accumulation during data presentation may enable improved structural probing on glycoproteins, with bTF as a proof-of-concept demonstration, featuring the unbiased structural sampling while maintaining nativelike structural information at a minimal cost of instrument time.

The CCS_{acc}-based data analysis method was further employed to assess its broad utility and versatility using a variety of glycoproteins up to 150 kDa with charge state distributions ranging from two to more than four major charges (Figures S2–S5). The proteins evaluated include α-chymotrypsin (Figure S2, 25 kDa), lactotransferrin (LTF, Figure S3, 83 kDa), albumin from chicken egg white (OVA, Figure S4, 43 kDa), and immunoglobulin G (IgG, Figure S5, 150 kDa). Data indicates that CCS_{acc}-derived unfolding fingerprints do not generate significantly different conformational information compared to individual charge states for low domain number/unfolding transition proteins with only two major charge states, such as α-chymotrypsin (Figure S2) and LTF (Figure S3). Notably, the CCSacc-derived fingerprints of the protein LTF allude to the presence of two coexisting conformations at high activation energy. Conflicting distinct fingerprints are observed from individual charge state-derived fingerprints of the protein OVA (Figure S4) with three observed major charge states, while CCS_{acc} operation summarizes and bridges this type of variation. We also tested the use of AIU and CCS_{acc} with a more complicated protein system, IgG, with more than four major charge states observed (Figure S5). Surprisingly, the CCS_{acc}-derived IgG datasets show some extent of differences to the most abundant

charge state-based datasets, in terms of both feature CCS distributions (Figure S5g) and conformational stability-linked CIU50 distributions (Figure S5h).

During AIU analysis, however, interference peaks can arise that are attributed to the charge stripping of the native ions to a lower charge state. The charge stripping phenomenon observed during IMS-MS analysis was evaluated using antibodies by Vallejo et al. where they noted that charge stripping occurs predictably based on charge state, with lesser charged ions experiencing reduced charge stripping⁴⁴. In addition, our recent application of AIU to sialylated glycoproteins independently support the limited influence of charge stripping on certain systems⁵³. Based on these observations, we expect the interference of charge stripped products to be limited to below 5% of the intensity of the precursor ion, which might not be the contributing factors preventing the further application of CCS_{acc} and AIU strategy, although this basically requires many more practices and validations adding to the proof-of-concept demonstration of the current study. To this end, we recommend performing a pre-test for potential charge stripping effects would be a practical solution for broader application of AIU and CCS_{acc} algorithm.

CONCLUSION

In this study, we compared the difference between two different unfolding data sampling strategies, namely CIU with quadrupole selection and AIU without quadrupole selection. This is followed by a new CCS data presentation means, CCS_{acc}, which summarizes all structural information across all observed charge states. This data integration method can be used with proteins over a wide mass range, although it is less informative for proteins with only single domain.

To show the potential benefits of CCS_{acc}, especially in terms of structural information, across a wide range of protein systems, we made a series of bar charts (Figures 3p-r, Figures 4h-i, Figures S2f-g, S3h-i, S4h-i, S5g-h), listing the feature CCS values and CIU50 values derived from individual charge states versus CCS_{acc} datasets. Our data indicates that, while CCS_{acc} fingerprints carries comparable structural information with individual charge states in simple protein systems with two main charge states (Figure S2 and S4), CCS_{acc} fingerprint surprisingly delivers varied structural information compared with most abundant charge state in protein systems with three or more major charge states (Figures 2/3, Figures S3/S5). Traditional CIU-based conformational analysis frequently and arbitrarily involves choosing the most abundant charge state to infer any potential structural and conformational information. Therefore, our data and observations support the utility of CCS_{acc}-based dataset in providing more structurally informative evidence compared with individual charge state-derived dataset, especially for relatively larger protein systems with wider charge state distributions. The enhanced capability enabled by CCS_{acc} fingerprint has been further validated when comparing two structurally similar proteins BSA and HSA, e.g. CCS_{acc}-based datasets enables the elevation of both delta CIU50 values (Figure 3q) and RMSD values (Figure 3r) by around ~6% compared to single charge state-derived datasets.

Our comparative datasets reveal that simultaneously operating, monitoring, and reporting all ions generated from a single protein can be generally beneficial for the continuous

development of time cost-effective, unfolding-based structural MS strategy, which is capable of sampling most of protein conformational species derived from solution phase. Consequently, a more sensitive analysis is achieved by accounting all ion species' conformational information. We envision that the CCS_{acc} strategy can find many more applications with improved signal-to-noise ratio of unfolding fingerprints and enriched information of topological structures as it can additionally better preserve nativelike conformers and tolerate more charge state fluctuations due to either instrumental conditions or protein charge state alteration in solution.

Supplementary Material

Refer to Web version on PubMed Central for supplementary material.

ACKNOWLEDGEMENTS

This work was funded in part by the NIH (R01DK071801, R56DK071801, RF1AG052324, and R21AG065728), and the NSF (CHE-2108223, CHE-1808541). A.P. was supported in part by the NIH Chemistry-Biology Interface Training Grant (T32 GM008505). L.L. acknowledges a Vilas Distinguished Achievement Professorship and Charles Melbourne Johnson Distinguished Chair Professorship with funding provided by the Wisconsin Alumni Research Foundation and University of Wisconsin-Madison School of Pharmacy. G.L. thanks the Nankai University start-up funding support through the Fundamental Research Funds for the Central Universities (No. 020/63213057).

REFERENCES

- 1. Fenn LS; Kliman M; Mahsut A; Zhao SR; McLean JA, Characterizing ion mobility-mass spectrometry conformation space for the analysis of complex biological samples. Anal. Bioanal. Chem 2009, 394 (1), 235–44. [PubMed: 19247641]
- 2. Paglia G; Kliman M; Claude E; Geromanos S; Astarita G, Applications of ion-mobility mass spectrometry for lipid analysis. Anal. Bioanal. Chem 2015, 407 (17), 4995–5007. [PubMed: 25893801]
- 3. Bohrer BC; Merenbloom SI; Koeniger SL; Hilderbrand AE; Clemmer DE, Biomolecule analysis by ion mobility spectrometry. Annu. Rev. Anal. Chem. (Palo Alto Calif) 2008, 1, 293–327. [PubMed: 20636082]
- 4. McLean JA; Ruotolo BT; Gillig KJ; Russell DH, Ion mobility–mass spectrometry: a new paradigm for proteomics. Int. J. Mass Spectrom 2005, 240 (3), 301–315.
- 5. Harvey SR; Macphee CE; Barran PE, Ion mobility mass spectrometry for peptide analysis. Methods 2011, 54 (4), 454–61. [PubMed: 21669288]
- 6. Uetrecht C; Rose RJ; van Duijn E; Lorenzen K; Heck AJ, Ion mobility mass spectrometry of proteins and protein assemblies. Chem. Soc. Rev 2010, 39 (5), 1633–55. [PubMed: 20419213]
- 7. Stauber J; MacAleese L; Franck J; Claude E; Snel M; Kaletas BK; Wiel IM; Wisztorski M; Fournier I; Heeren RM, On-tissue protein identification and imaging by MALDI-ion mobility mass spectrometry. J. Am. Soc. Mass Spectrom 2010, 21 (3), 338–47. [PubMed: 19926301]
- 8. Ruotolo BT; Benesch JL; Sandercock AM; Hyung SJ; Robinson CV, Ion mobility-mass spectrometry analysis of large protein complexes. Nat. Protoc 2008, 3 (7), 1139–52. [PubMed: 18600219]
- Niu S; Ruotolo BT, Collisional unfolding of multiprotein complexes reveals cooperative stabilization upon ligand binding. Protein. Sci 2015, 24 (8), 1272–81. [PubMed: 25970849]
- Hopper JT; Oldham NJ, Collision induced unfolding of protein ions in the gas phase studied by ion mobility-mass spectrometry: the effect of ligand binding on conformational stability. J. Am. Soc. Mass Spectrom 2009, 20 (10), 1851–8. [PubMed: 19643633]
- 11. Zhong Y; Han L; Ruotolo BT, Collisional and Coulombic unfolding of gas-phase proteins: high correlation to their domain structures in solution. Angew. Chem., Int. Ed 2014, 53 (35), 9209–12.

12. Huang Y; Salinas ND; Chen E; Tolia NH; Gross ML, Native Mass Spectrometry, Ion mobility, and Collision-Induced Unfolding Categorize Malaria Antigen/Antibody Binding. J. Am. Soc. Mass Spectrom 2017, 28 (11), 2515–2518. [PubMed: 28875466]

- Smith RD; Loo JA; Edmonds CG; Barinaga CJ; Udseth HR, New developments in biochemical mass spectrometry: electrospray ionization. Anal. Chem 1990, 62 (9), 882–99. [PubMed: 2194402]
- 14. Chowdhury SK; Katta V; Chait BT, Probing conformational changes in proteins by mass spectrometry. J. Am. Chem. Soc 1990, 112 (24), 9012–9013.
- 15. Testa L; Brocca S; Santambrogio C; D'Urzo A; Habchi J; Longhi S; Uversky VN; Grandori R, Extracting structural information from charge-state distributions of intrinsically disordered proteins by non-denaturing electrospray-ionization mass spectrometry. Intrinsically Disord. Proteins 2013, 1 (1), e25068. [PubMed: 28516012]
- 16. Loo JA; Edmonds CG; Udseth HR; Smith RD, Effect of reducing disulfide-containing proteins on electrospray ionization mass spectra. Anal. Chem 1990, 62 (7), 693–8. [PubMed: 2327585]
- Amad MH; Cech NB; Jackson GS; Enke CG, Importance of gas-phase proton affinities in determining the electrospray ionization response for analytes and solvents. J. Mass Spectrom 2000, 35 (7), 784–9. [PubMed: 10934432]
- 18. Fenn JB, Ion formation from charged droplets: Roles of geometry, energy, and time. J. Am. Soc. Mass Spectrom 1993, 4 (7), 524–35. [PubMed: 24227639]
- 19. Kaltashov IA; Eyles SJ, Studies of biomolecular conformations and conformational dynamics by mass spectrometry. Mass Spectrom. Rev 2002, 21 (1), 37–71. [PubMed: 12210613]
- Wang G; Cole RB, Effect of Solution Ionic Strength on Analyte Charge State Distributions in Positive and Negative Ion Electrospray Mass Spectrometry. Anal. Chem 2002, 66 (21), 3702– 3708.
- Guevremont R; Siu KWM; Blanc JCY; Berman SS, Are the electrospray mass spectra of proteins related to their aqueous solution chemistry? J. Am. Soc. Mass Spectrom 1992, 3 (3), 216–224.
 [PubMed: 24242944]
- Zhao C; Wood TD; Bruckenstein S, Shifts in protein charge state distributions with varying redox reagents in nanoelectrospray triple quadrupole mass spectrometry. J. Am. Soc. Mass Spectrom 2005, 16 (3), 409–16. [PubMed: 15734335]
- 23. Fisher CM; Kharlamova A; McLuckey SA, Affecting protein charge state distributions in nanoelectrospray ionization via in-spray solution mixing using theta capillaries. Anal. Chem 2014, 86 (9), 4581–8. [PubMed: 24702054]
- 24. Le Blanc JCY; Wang J; Guevremont R; Siu KWM, Electrospray mass spectra of protein cations formed in basic solutions. Org. Mass Spectrom 1994, 29 (11), 587–593.
- 25. Susa AC; Xia Z; Tang HYH; Tainer JA; Williams ER, Charging of Proteins in Native Mass Spectrometry. J. Am. Soc. Mass Spectrom 2017, 28 (2), 332–340. [PubMed: 27734326]
- 26. Kelly MA; Vestling MM; Fenselau CC; Smith PB, Electrospray analysis of proteins: A comparison of positive-ion and negative-ion mass spectra at high and low pH. Org. Mass Spectrom 1992, 27 (10), 1143–1147.
- 27. Iavarone AT; Williams ER, Mechanism of charging and supercharging molecules in electrospray ionization. J. Am. Chem. Soc 2003, 125 (8), 2319–27. [PubMed: 12590562]
- 28. Chillier XFD; Monnier A; Bill H; Gülaçar FO; Buchs A; McLuckey SA; Van Berkel GJ, A Mass Spectrometry and Optical Spectroscopy Investigation of Gas-phase Ion Formation in Electrospray. Rapid Commun. Mass Spectrom 1996, 10 (3), 299–304.
- 29. Iavarone AT; Jurchen JC; Williams ER, Effects of solvent on the maximum charge state and charge state distribution of protein ions produced by electrospray ionization. J. Am. Soc. Mass Spectrom 2000, 11 (11), 976–85. [PubMed: 11073261]
- 30. McAllister RG; Metwally H; Sun Y; Konermann L, Release of Native-like Gaseous Proteins from Electrospray Droplets via the Charged Residue Mechanism: Insights from Molecular Dynamics Simulations. J. Am. Chem. Soc 2015, 137 (39), 12667–76. [PubMed: 26325619]
- 31. Carbeck JD; Severs JC; Gao J; Wu Q; Smith RD; Whitesides GM, Correlation between the Charge of Proteins in Solution and in the Gas Phase Investigated by Protein Charge Ladders, Capillary

- Electrophoresis, and Electrospray Ionization Mass Spectrometry. J. Phys. Chem. B 1998, 102 (51), 10596–10601.
- 32. Heck AJ; Van Den Heuvel RH, Investigation of intact protein complexes by mass spectrometry. Mass Spectrom. Rev 2004, 23 (5), 368–89. [PubMed: 15264235]
- 33. van den Heuvel RH; Heck AJ, Native protein mass spectrometry: from intact oligomers to functional machineries. Curr. Opin. Chem. Biol 2004, 8 (5), 519–26. [PubMed: 15450495]
- 34. Benesch JL; Robinson CV, Mass spectrometry of macromolecular assemblies: preservation and dissociation. Curr. Opin. Struct. Biol 2006, 16 (2), 245–51. [PubMed: 16563743]
- 35. Breuker K; McLafferty FW, Stepwise evolution of protein native structure with electrospray into the gas phase, 10(-12) to 10(2) s. Proc. Natl. Acad. Sci. U. S. A 2008, 105 (47), 18145-52. [PubMed: 19033474]
- 36. Scarff CA; Thalassinos K; Hilton GR; Scrivens JH, Travelling wave ion mobility mass spectrometry studies of protein structure: biological significance and comparison with X-ray crystallography and nuclear magnetic resonance spectroscopy measurements. Rapid Commun. Mass Spectrom 2008, 22 (20), 3297–304. [PubMed: 18816489]
- 37. Wang G; Cole RB, Disparity between solution-phase equilibria and charge state distributions in positive-ion electrospray mass spectrometry. Org. Mass Spectrom 1994, 29 (8), 419–427.
- 38. Wyttenbach T; Bowers MT, Structural stability from solution to the gas phase: native solution structure of ubiquitin survives analysis in a solvent-free ion mobility-mass spectrometry environment. J. Phys. Chem. B 2011, 115 (42), 12266–75. [PubMed: 21905704]
- 39. Bernstein SL; Wyttenbach T; Baumketner A; Shea JE; Bitan G; Teplow DB; Bowers MT, Amyloid beta-protein: monomer structure and early aggregation states of Abeta42 and its Pro19 alloform. J. Am. Chem. Soc 2005, 127 (7), 2075–84. [PubMed: 15713083]
- Fantin SM; Parson KF; Niu S; Liu J; Polasky DA; Dixit SM; Ferguson-Miller SM; Ruotolo BT, Collision Induced Unfolding Classifies Ligands Bound to the Integral Membrane Translocator Protein. Anal. Chem 2019, 91 (24), 15469–15476. [PubMed: 31743004]
- Fantin SM; Huang H; Sanders CR; Ruotolo BT, Collision-Induced Unfolding Differentiates Functional Variants of the KCNQ1 Voltage Sensor Domain. J. Am. Soc. Mass Spectrom 2020, 31 (11), 2348–2355. [PubMed: 32960579]
- 42. Laganowsky A; Reading E; Allison TM; Ulmschneider MB; Degiacomi MT; Baldwin AJ; Robinson CV, Membrane proteins bind lipids selectively to modulate their structure and function. Nature 2014, 510 (7503), 172–175. [PubMed: 24899312]
- 43. Gadkari VV; Ramirez CR; Vallejo DD; Kurulugama RT; Fjeldsted JC; Ruotolo BT, Enhanced Collision Induced Unfolding and Electron Capture Dissociation of Native-like Protein Ions. Anal. Chem 2020, 92 (23), 15489–15496. [PubMed: 33166123]
- 44. Vallejo DD; Polasky DA; Kurulugama RT; Eschweiler JD; Fjeldsted JC; Ruotolo BT, A Modified Drift Tube Ion Mobility-Mass Spectrometer for Charge-Multiplexed Collision-Induced Unfolding. Anal. Chem 2019, 91 (13), 8137–8146. [PubMed: 31194508]
- 45. Polasky DA; Dixit SM; Vallejo DD; Kulju KD; Ruotolo BT, An Algorithm for Building Multi-State Classifiers Based on Collision-Induced Unfolding Data. Anal. Chem 2019, 91 (16), 10407–10412. [PubMed: 31310505]
- 46. Donor MT; Shepherd SO; Prell JS, Rapid Determination of Activation Energies for Gas-Phase Protein Unfolding and Dissociation in a Q-IM-ToF Mass Spectrometer. J. Am. Soc. Mass Spectrom 2020, 31 (3), 602–610. [PubMed: 32126776]
- 47. Bush MF; Hall Z; Giles K; Hoyes J; Robinson CV; Ruotolo BT, Collision Cross Sections of Proteins and Their Complexes: A Calibration Framework and Database for Gas-Phase Structural Biology. Anal. Chem 2010, 82 (22), 9557–9565. [PubMed: 20979392]
- Polasky DA; Dixit SM; Vallejo DD; Kulju KD; Ruotolo BT, An Algorithm for Building Multi-State Classifiers Based on Collision-Induced Unfolding Data. Anal. Chem 2019, 91 (16), 10407– 10412. [PubMed: 31310505]
- 49. Polasky DA; Dixit SM; Fantin SM; Ruotolo BT, CIUSuite 2: Next-Generation Software for the Analysis of Gas-Phase Protein Unfolding Data. Anal. Chem 2019, 91 (4), 3147–3155. [PubMed: 30668913]

50. Eschweiler JD; Martini RM; Ruotolo BT, Chemical Probes and Engineered Constructs Reveal a Detailed Unfolding Mechanism for a Solvent-Free Multidomain Protein. J. Am. Chem. Soc 2017, 139 (1), 534–540. [PubMed: 27959526]

- 51. Eschweiler JD; Rabuck-Gibbons JN; Tian Y; Ruotolo BT, CIUSuite: A Quantitative Analysis Package for Collision Induced Unfolding Measurements of Gas-Phase Protein Ions. Anal. Chem 2015, 87 (22), 11516–11522. [PubMed: 26489593]
- 52. Wada Y, Mass spectrometry of transferrin glycoforms to detect congenital disorders of glycosylation: Site-specific profiles and pitfalls. Proteomics 2016, 16 (24), 3105–3110. [PubMed: 27095603]
- 53. Li G; Phetsanthad A; Ma M; Yu Q; Nair A; Zheng Z; Ma F; DeLaney K; Hong S; Li L, Native Ion Mobility-Mass Spectrometry-Enabled Fast Structural Interrogation of Labile Protein Surface Modifications at the Intact Protein Level. Anal. Chem 2022, 94 (4), 2142–2153. [PubMed: 35050568]

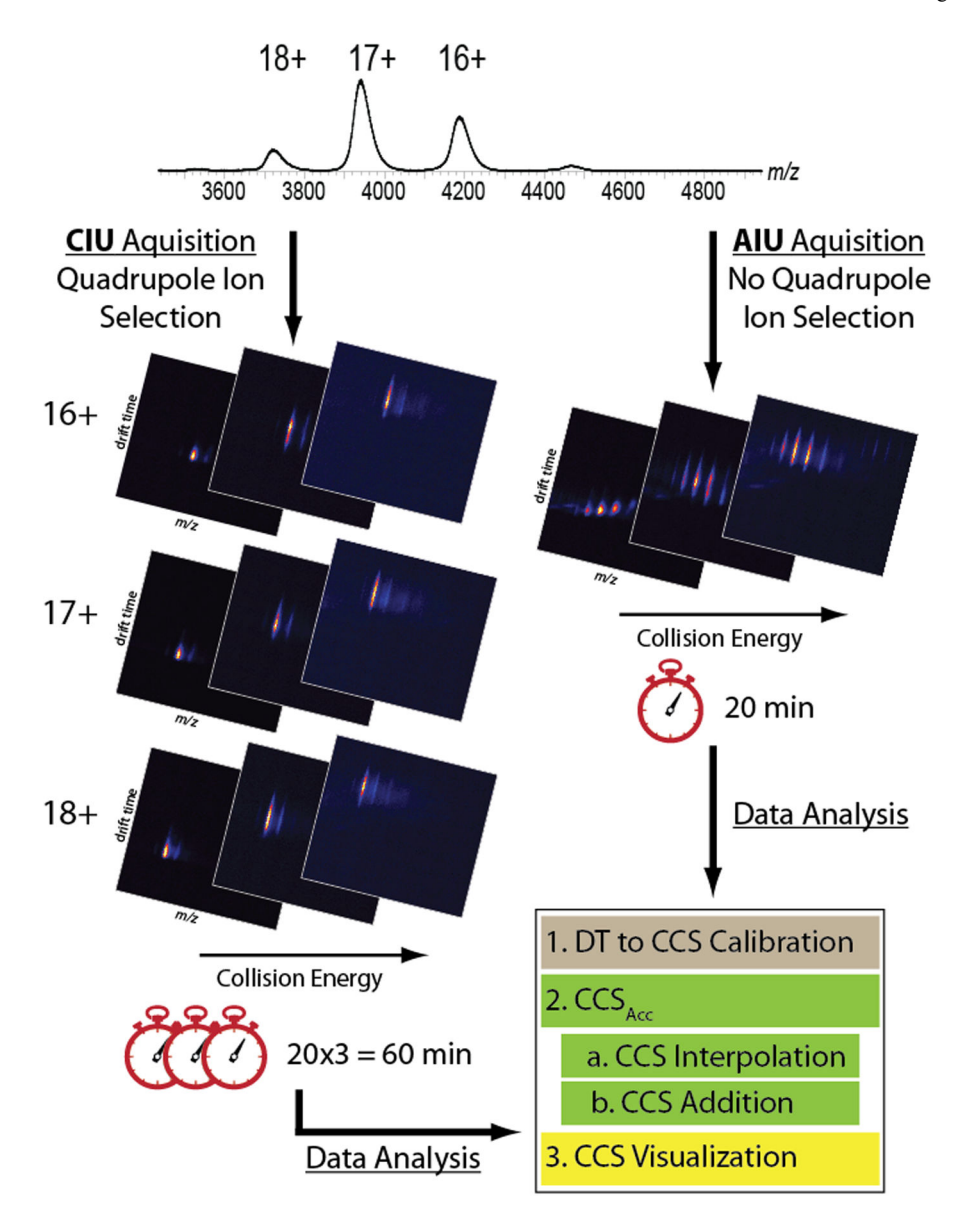


Figure 1.

Comparative overview of AIU and CIU workflows with the incorporation of CCS accumulation. Starting with the same native IM-MS datasets, while traditional CIU workflow involves the isolation of each individual charge state over a range of collision voltages, AIU workflow requires only one iteration of collision voltage ramping. For data analysis, a new CCS interpolation and integration method is introduced for both AIU and CIU datasets.

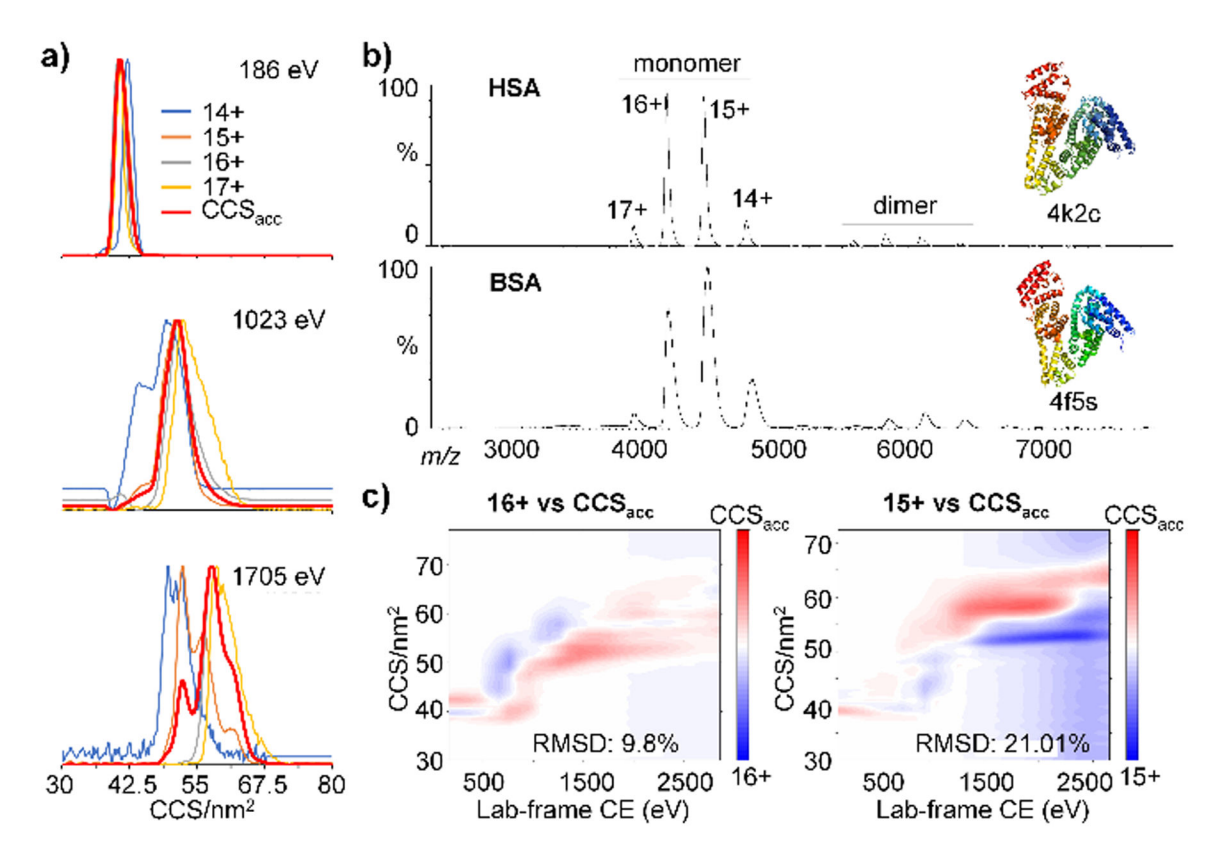


Figure 2. CCS $_{acc}$ -enabled comprehensive structural analysis. (a) Representative CCS $_{acc}$ distribution profiles of HSA at several unfolding voltages (lab-frame CE: 186 eV (top), 1023 eV (middle), 1705 eV (bottom)) generated through relative intensity-determined contributions. (b) Representative mass spectra for HSA and BSA used for intensity pickup. (c) Difference plots between HSA 16+ and 15+ (two most abundant) and CCS $_{acc}$ unfolding fingerprints.

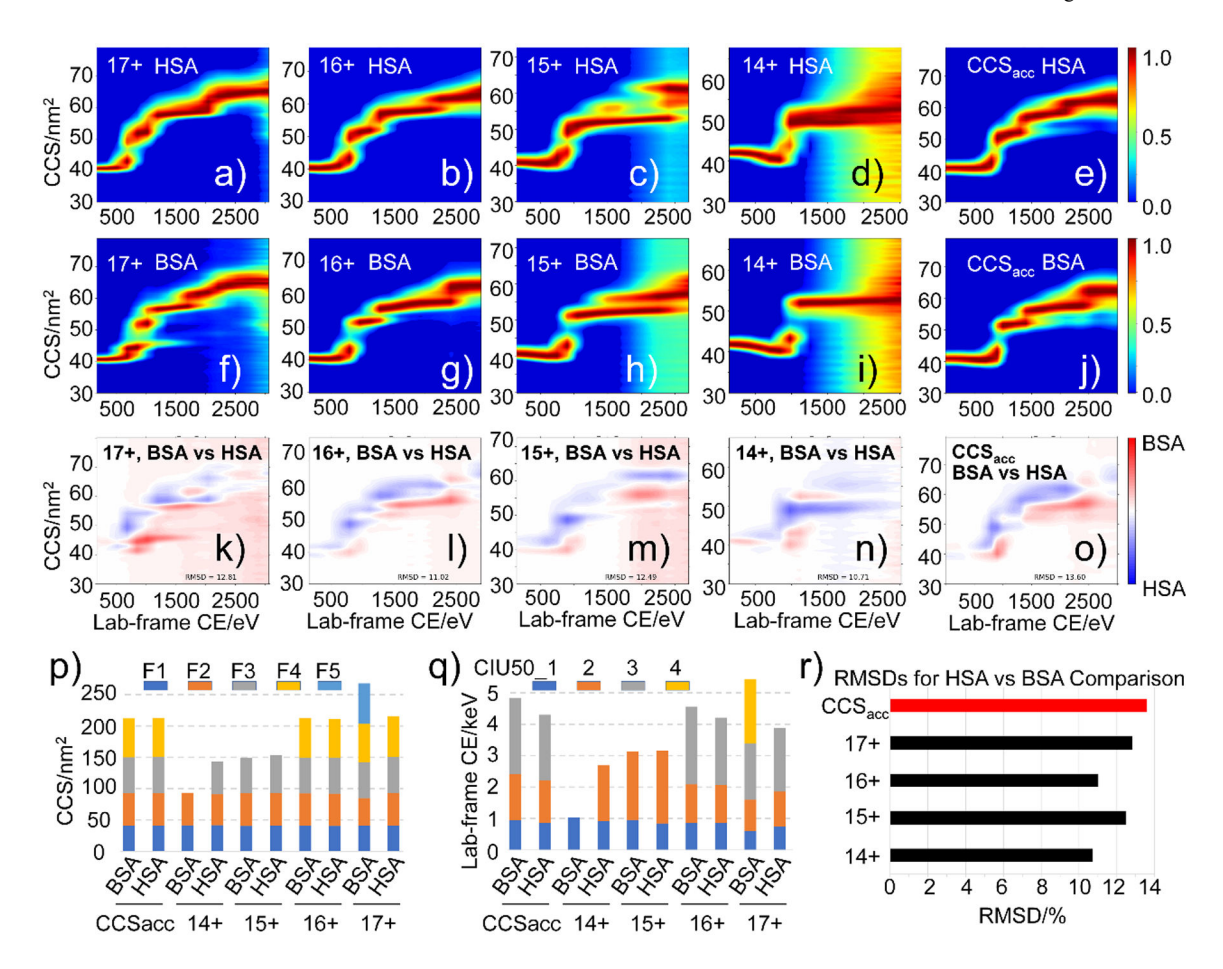


Figure 3.

CCS_{acc} as a tool for comprehensive structural comparison between HSA and BSA.

Unfolding fingerprints for individual charge states and for accumulated CCS datasets generated of (a-e) HSA and (f-j) BSA as well as (k-o) difference plots between the two species with RMSD values: 12.81%, 11.02%, 12.49%, 10.71% and 13.60%. Feature CCS, CIU₅₀ values, and corresponding RMSD values were also shown in p, q and r, respectively.

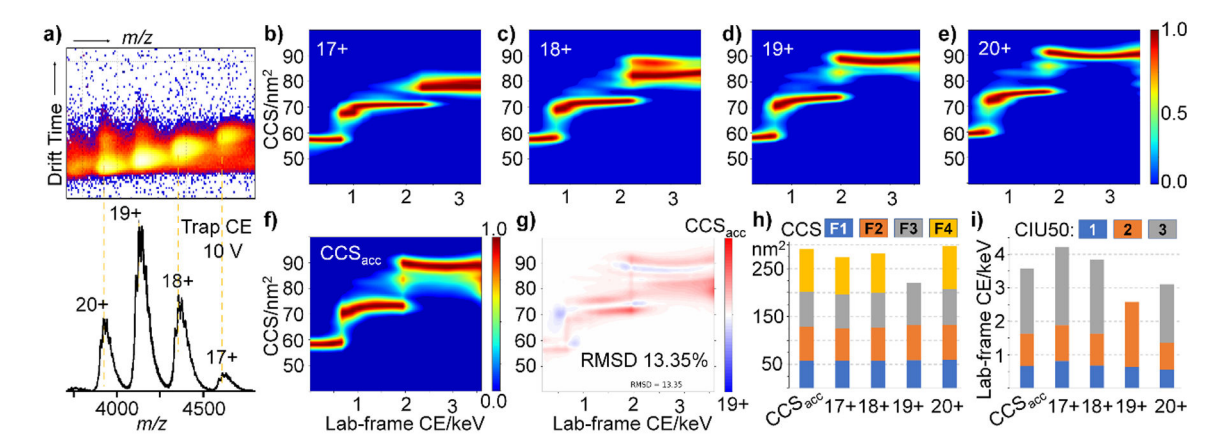


Figure 4. Improved structural probing on sialylated glycoprotein via CCS_{acc}. (a) Representative mass spectra and corresponding IM heatmap showing charge states from 20+ to 17+ of bTF under gentle condition (10 V). Stepwise unfolding fingerprints of bTF of (b-e) individual charge states and (f) accumulated CCS are shown along with (g) the difference plot between the most abundant charge state and CCS_{acc}. (h) Feature CCS and (i) CIU₅₀ values are shown for each data set.